I.J. Image, Graphics and Signal Processing, **2023, 5, 1-16**
Published Online on October 8, 2023 by MECS Press (http://www.mecs-press.org/)
DOI: 10.5815/ijigsp.2023.05.01

Image Denoising based on Enhanced Wavelet Global Thresholding Using Intelligent Signal Processing Algorithm

Joseph Isabona
Department of Physics, Federal University Lokoja, Lokoja 260101, Nigeria
Email: joseph.isabona@fulokoja.edu.ng
ORCID: https://orcid.org/0000-0002-2606-4315

Agbotiname Lucky Imoize*
Department of Electrical and Electronics Engineering, Faculty of Engineering, University of Lagos, Akoka, Lagos 100213, Nigeria
Email: aimoize@unilag.edu.ng
ORCID: https://orcid.org/0000-0001-8921-8353
*Corresponding Author

Stephen Ojo
Department of Electrical and Computer Engineering, College of Engineering, Anderson University, Anderson, SC 29621, USA
Email: sojo@andersonuniversity.edu
ORCID: https://orcid.org/0000-0002-2383-621X

Received: 2 April 2023; Revised: 02 June 2023; Accepted: 30 June 2023; Published: 08 October 2023

Abstract: Denoising is a vital aspect of image preprocessing, often explored to eliminate noise in an image to restore its proper characteristic formation and clarity. Unfortunately, noise often degrades the quality of valuable images, making them meaningless for practical applications. Several methods have been deployed to address this problem, but the quality of the recovered images still requires enhancement for efficient applications in practice. In this paper, a wavelet-based universal thresholding technique that possesses the capacity to optimally denoise highly degraded noisy images with both uniform and non-uniform variations in illumination and contrast is proposed. The proposed method, herein referred to as the modified wavelet-based universal thresholding (MWUT), compared to three state-of-the-art denoising techniques, was employed to denoise five noisy images. In order to appraise the qualities of the images obtained, seven performance indicators comprising the Root Mean Square Error (RMSE), Mean Absolute Error (MAE), Structural Content (SC), Peak Signal to Noise Ratio (PSNR), Structural Similarity Index Method (SSIM), Signal-to-Reconstruction-Error Ratio (SRER), Blind Spatial Quality Evaluator (NIQE), and Blind/Referenceless Image Spatial Quality Evaluator (BRISQUE) were employed. The first five indicators – RMSE, MAE, SC, PSNR, SSIM, and SRER- are reference indicators, while the remaining two – NIQE and BRISQUE- are referenceless. For the superior performance of the proposed wavelet threshold algorithm, the SC, PSNR, SSIM, and SRER must be higher, while lower values of NIQE, BRISQUE, RMSE, and MAE are preferred. A higher and better value of PSNR, SSIM, and SRER in the final results shows the superior performance of our proposed MWUT denoising technique over the preliminaries. Lower NIQE, BRISQUE, RMSE, and MAE values also indicate higher and better image quality results using the proposed modified wavelet-based universal thresholding technique over the existing schemes. The modified wavelet-based universal thresholding technique would find practical applications in digital image processing and enhancement.

Index Terms: Wavelet transforms; Noisy image; Denoising; BRISQUE; Wavelet thresholding; Improved universal thresholding; Intelligent signal processing.

1. Introduction

Denoising remained a vital area of image preprocessing to remove noise from an image to restore its proper formation and nature [1–3]. Generally, effective image processing and storage often suffer major setbacks due to

various alterations created by noise during capture or acquisition and via electronic transmission [4,5]. For example, the film grain can be the main noise source if an image is captured and scanned employing a photograph made with a certain film during processing. Also, the noise can corrupt an acquired image using digital format by using a detector-based image data-gathering mechanism in the processing [6]. Thus, anything that interferes with and deteriorates the characteristics of the original image during acquisition, electronic transmission, reproduction, and storage is considered noise. The effective removal of this noisy component without losing the essential features of the original image and signal data is a challenging task [7–9], making it an active research area in recent times. The need to investigate this exciting area of research in the current study is not out of place. Therefore, this study proposes a modified universal wavelet-based thresholding (MWUT) method, which optimally denoises degraded noisy images with uniform and non-uniform variations in illumination and contrast.

The conventional means of image processing involving noise removal in the existing literature comprises averaging filters, Wiener filters, median filters, and the Fourier transform methods [10–19]. These methods are mainly based on low frequency-selective filters. However, these filters often fail once noise occupies or shares a parallel and comparable frequency band within the image. Another key disadvantage of most filters is their inability to mollify medium-tailed and related noise distributions [20–23].

Over the years, Fourier transforms and the other filtering techniques highlighted above have been deployed. However, another unique image and signal denoising technique, wavelet transforms, has become the first choice in modern literature due to its distinctive multi-resolution analysis and time-frequency localization advantages [24]. The wavelet transform can orthogonalize any image or data being processed and reproduces the sparse matrix transformation in the original image. It has been shown to outperform other image processing and transformation techniques [25,26]. The wavelet transform has two exceptional properties, which are scale and location. The scale, also commonly termed dilation, is the property that defines how crushed" or "stretched" the wavelet is in relationship to frequency. The location property determines how the wavelet is positioned in space or time. The two properties enable it to decompose images or data into coarse (approximation) levels and finer (detail) parts.

In previous works, a range of techniques based on wavelet theory exist, and the key ones include the wavelet threshold technique, modulus maxima technique, and wavelet correlation technique [27]. Among these techniques, the wavelet threshold technique proposed by Donoho and Johnstone [28] is the most extensively engaged owing to its simplified computational approach and weighty influence. However, the effectiveness of this technique depends on the suitable choice of its optimal threshold value when employed in noisy image-based preprocessing or denoising. Choosing too large a threshold value can filter out useful information in the image. On the other hand, if the selected threshold value is too small, it may retain a large amount of noise in the image. A comparative evolution of six wavelet thresholding techniques toward effective Image denoising was proposed [29]. Results indicate that the neigh shrink and block shrink sure provided the best wavelet-based thresholding compared to the four thresholding wavelet methods. Similarly, an improved wavelet thresholding approach that can give outstanding image processing details and quality is proposed and explored for wireless camera networks via computer simulation [30].

A new threshold function, Fleming, has been reported [31] for optimal PD signals treatment and preserved partial discharge analysis. Recently, an enriched threshold calculation scheme that considers different decomposition layers based on wavelet threshold has been proposed [32]. The sample application employed by the authors revealed that the proposed scheme can perfectly denoise and reserve the desired features of the processed signals. However, the above wavelet thresholding methods are only appropriate in uniformly illuminated noisy images with contrast distribution. Therefore, the above techniques could suffer severe limitations when substantial noise and non-uniform variation in illumination and contrast exist in noisy images [33–35].

To this end, this paper proposes the modified universal wavelet-based thresholding (MWUT) method, which optimally denoises degraded noisy images with uniform and non-uniform variations in illumination and contrast. The optimal performance quality of the proposed method is examined using practical examples compared to three state-of-the-art denoising techniques provided using seven distinctive performance gauges. These include the Root Mean Square Error (RMSE), Mean Absolute Error (MAE), Structural Content (SC), Peak Signal-to-Noise Ratio (PSNR), Structural Similarity Index Method (SSIM), Signal-to-Reconstruction-Error Ratio (SRER), Blind Spatial Quality Evaluator (NIQE), and Blind/Referenceless Image Spatial Quality Evaluator (BRISQUE).

In particular, the main contributions of this paper are outlined as follows:

- A modified universal threshold computation technique termed MWUT is proposed in this work.
- The noisy image denoising procedure is demonstrated using the proposed MWUT technique.
- A quantitative assessment of the denoised images is presented to examine the efficacy of the proposed wavelet-based threshold technique.

The remaining part of this paper is organized as follows. Section 2 presents the theory of wavelet thresholding and the universal wavelet-based thresholding algorithm. Section 3 describes the modified universal threshold computation algorithm and the noisy image denoising procedure using the proposed MWUT technique. Section 4 presents the results of the proposed algorithm and a quantitative assessment of the denoised images. Finally, Section 5 offers a concise conclusion to the study.

2. Wavelength Thresholding

Wavelet thresholding, called 'wavelet shrinkage', is a unique nonlinear technique of transforming or denoising an image to a time-scale domain by thresholding the wavelet coefficients.

Consider a situation during transmission and acquisition wherein noise acts upon an original image via direct superposition given by equation (1):

$$A(k) = B(k) + C(k) \tag{1}$$

where $B(k)$ and $A(k)$ express the respective original image and observed noisy image with $\mathrm{C}(k) \approx N(0, \sigma^2)$ denoting the noise distribution at the acquisition (receiver) end. In wavelet transform analysis, denoising is accomplished by thresholding. The foremost step is to estimate the original image $B(k)$ from the noisy image $A(k)$ with minimum error.

Let W_d indicate a $M \times M$discrete wavelet transform matrix and W_d^{-1}, the wavelet transforms inverse. Applying the wavelet transform on equation (1) results in equation (2):

$$Q = R + Z \tag{2}$$

where $Q = W_d(A)$ expresses the image wavelet coefficients, $R = W_d(B)$, $Z = W_d(C)$

The above process is such that by applying the wavelet transform on the image and then subjecting it through a threshold, the larger entries Q are retained while removing or shrinking the noisy component below a fixed value. Then, the inverse transform of the denoised estimate is given by equation (3):

$$f = W_d^{-1} Q \tag{3}$$

2.1. Universal Wavelet-based Thresholding

Different approaches exist for wavelet-based thresholding, all producing different results when applied to signals or images during processing. Generally, the different techniques can be grouped as soft, semi-soft, or hard thresholding. The universal threshold, also known as Visushrink, was originally proposed and applied by Donoho [27,28]. It is given by equation (4), and the noise variance is given by equation (5):

$$\lambda_G = \hat{\sigma}\sqrt{2.log(N)} \tag{4}$$

$$\hat{\sigma} = \sqrt{2}[\text{median}(|\text{w-median}(w)|)]\ /.6745 \tag{5}$$

where $N$is the sampling points number (or length), and median(|w−median(w)|) defines the wavelet coefficient median absolute deviation, with w expressing the vector of wavelet coefficients. Equation (5), $\hat{\sigma}$ estimates the noise variance. The above thresholding approach can flop once the contextual radiance of the image is uneven. The resultant effect is a poor and imprecise reconstruction of the desired processed image, a major weakness.

3. Proposed Methodology

This section presents the proposed wavelet-based thresholding technique, the noisy image denoising procedure using the proposed MWUT, and a quantitative assessment of the proposed MWUT technique.

3.1. The proposed Wavelet-based Thresholding Technique

A modified universal threshold computation formula termed MWUT is proposed in this work. As shown in equation (6), a constant term *z* that can improve the original universal threshold computation formula is introduced, and it is given by equation (7):

$$\lambda_{MUT} = z * \hat{\sigma}\sqrt{2.log(N)} \tag{6}$$

$$z = 1/\log 10(\text{prod}\ (\text{size}(X))) \tag{7}$$

Here, λ_{MUT} indicates the modified universal threshold formula, and the parameter z is introduced to regulate the properties of the image size X being denoised.

For $z = 1$, the modified universal threshold formula reduces to a threshold value of equation (8), i.e.:

$$\lim_{z \to 1} \lambda_{MUT} = z * \hat{\sigma}\sqrt{2.log(N)} \tag{8}$$

where $\hat{\sigma}$ estimates the noise standard deviation.

As demonstrated in Fig. 1 using a flow block diagram, the modified universal threshold is applied to the noisy image by following algorithm 1 described in the next section.

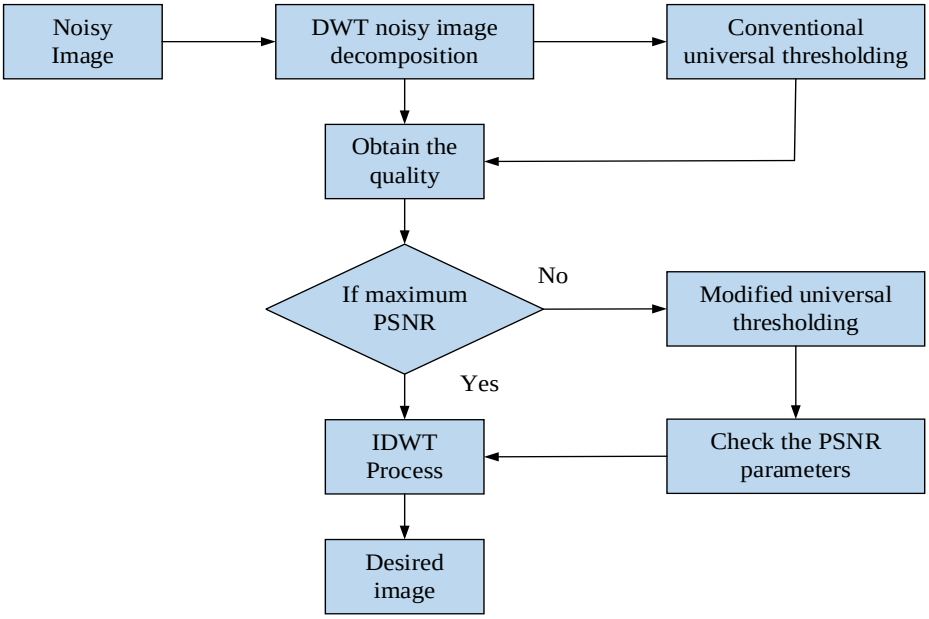

Fig. 1. Modified universal threshold computation method

3.2. The Denoising Algorithm

The stepwise image denoising procedure, tagged algorithm 1, is designed to achieve a near-optimal wavelet-based soft thresholding in the denoising algorithm. The algorithm is reasonably simple and computationally efficient to implement. It has the following steps as given in algorithm 1.

Algorithm 1: **The noisy image denoising procedure using the proposed MWUT**

Step 1: **Input:** Noisy image; **Resultant output:** Desired image
Step 2: Add Gaussian white noise to the image to obtain the noisy image
Step 3: Use the DWT to decompose the noisy image
Step 4: Calculate the noise variance
Step 5: Calculate the actual noisy image ratio using equation (5)
Step 6: Multiply the computed actual noisy image ratio with the convention universal threshold to obtain the modified universal threshold
Step 7: Denoised the noisy image with the modified universal threshold
Step 8: Reconstruct using IDWT to obtain the desired image
Step 9: Appraise the desired image quality using key performance metrics like PSNR, SSIM, NIQE, etc.

3.3. Quantitative Assessment Indicators

The image quality indicators considered to assess the efficacy of the proposed wavelet-based threshold technique include the Root Mean Square Error (RMSE) [36–38], Mean Absolute Error (MAE) [39–41], Structural Content (SC) [42], Peak Signal to Noise ratio (PSNR) [43], Structural Similarity Index Method (SSIM) [44], Blind Spatial Quality Evaluator (NIQE) [45,46], Signal-to-Reconstruction-Error Ratio (SRER) [47] and Blind/Referenceless Image Spatial Quality Evaluator (BRISQUE) [48,49]. Assuming the error between the reconstructed desired image $b(k)$ and the original image $a(k)$ is $e(k) = a(k) - b(k), k = 0,1,2,3,\ldots, K-1$, then the RMSE, MAE, SC, PSNR, SRER, and SSIM can be expressed as given in equations (9)-(14):

$$RMSE = \left[\frac{1}{K}\sum_{k=0}^{K-1} e(k)^2\right]^{0.5} \tag{9}$$

$$MAE = \frac{\sum_{k=0}^{K-1}|e(k)|}{K} \tag{10}$$

$$SC = \frac{\sum_{k=0}^{k-1}(a(k))^2}{\sum_{k=0}^{k-1}(b(k))^2} \tag{11}$$

$$PSNR = \left\{\frac{S_{Max}^2}{\sum_{k=0}^{K-1}|e(k)|}\right\} \tag{12}$$

$$SRER = \frac{E\|a(k)\|^2}{E\|a(k)-a(k)\|^2} \tag{13}$$

$$SSIM(x,y) = [l(a,b)]^o \times [c(a,b)]^p \times [s(a,b)]^q \tag{14}$$

where S_{Max} signifies the maximum image pixel intensity value. In equation (14), the $l(a,b)$, $c(a,b)$, and $s(a,b)$ denote the luminance intensity term, contrast configuration term, and local structure formation term, with o, p, and q being positive constants [e.g., $o = p = q = 1$] [50]. The BRISQUE is a subjective indicator for assessing opinion-aware image quality, and the NIQE is an *opinion-unaware* indicator that measures the naturalness of the image quality.

4. Results and Discussions

The efficacy of the proposed threshold technique is comparatively evaluated over the standard universal threshold and other critical state-of-the-art filters, such as the median and averaging filters. The experimental evaluation is actualized with noisy color images of 256 x 256 pixels, and each image is processed at 5, 10, 15, and 20dB white Gaussian noise levels. The proposed threshold technique was compared with other techniques using MATLAB. Furthermore, Symlet wavelet sifts at level 2 decomposition level is used to conduct the efficacy of the proposed method. Our earlier works show the precedure and methods used in the current study more clearly to ease research reproduction [7–9]. Figs. 1a and 1b, 2a and 2b, 3a and 3b, 4a and 4b, respectively, displayed the original and noisy images being processed. Figs. 1c to 1f, 2c and 2f, 3c and 3f, 4a and 4f present the results of the processed images using the proposed thresholding technique compared with the standard universal threshold and other critical state-of-the-art filters. Figs. 2 to 6 are the original, noisy, and denoised Mask, Mandrill, Sinsin, Cathe_1, and Bust images, respectively, using the proposed modified wavelet-based universal thresholding technique compared with other conventional methods. The images in Figs. 2a and 2b, 3a and 3b, 4a and 4b, 5a, 5b and 6a, and 6b are displayed to reveal the original and input noisy images. In contrast, the images in Figs. 2c to 2f, 3c to 3f, 4c to 4f, 5c to 5f, and 6c to 6f are displayed to show their resultant image using the proposed modified wavelet-based universal thresholding and conventional wavelet-based universal thresholding, median filter and averaging filter [16,17].

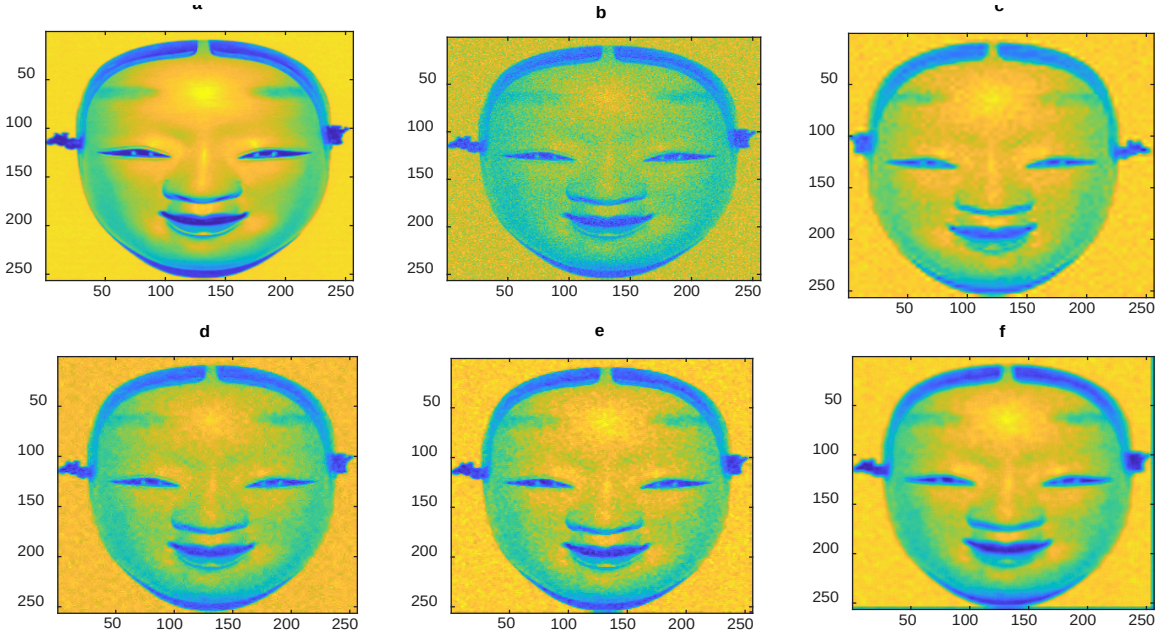

Fig. 2. Comparison of different denoising techniques on Mask Images. a) Original images. b) Input Noisy image. c) Denoised image using conventional wavelet-based universal thresholding [27,28]. d) Denoised image using Proposed modified wavelet-based universal thresholding. e) Denoised image using median filter [13–15]. f) Denoised image using averaging filtering [16,17].

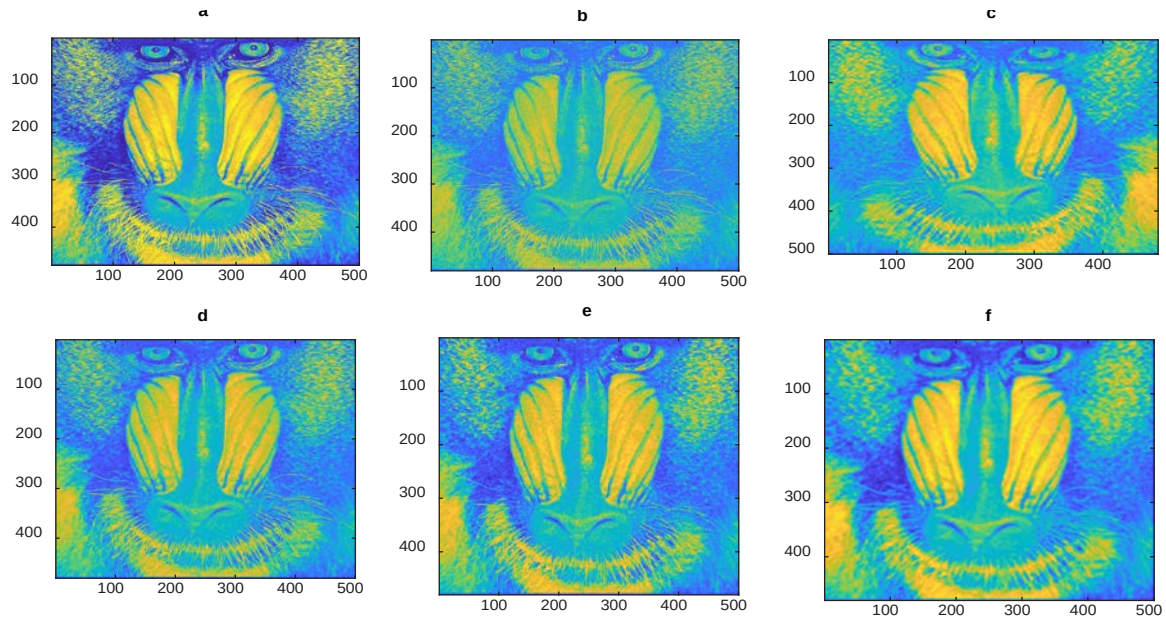

Fig. 3. Comparison of different denoising techniques on Mandrill Image. a) Original images. b) Input Noisy image. c) Denoised image using conventional wavelet-based universal thresholding [27,28]. d) Denoised image using Proposed modified wavelet-based universal thresholding. e) Denoised image using median filter [13–15]. f) Denoised image using averaging filtering [16,17].

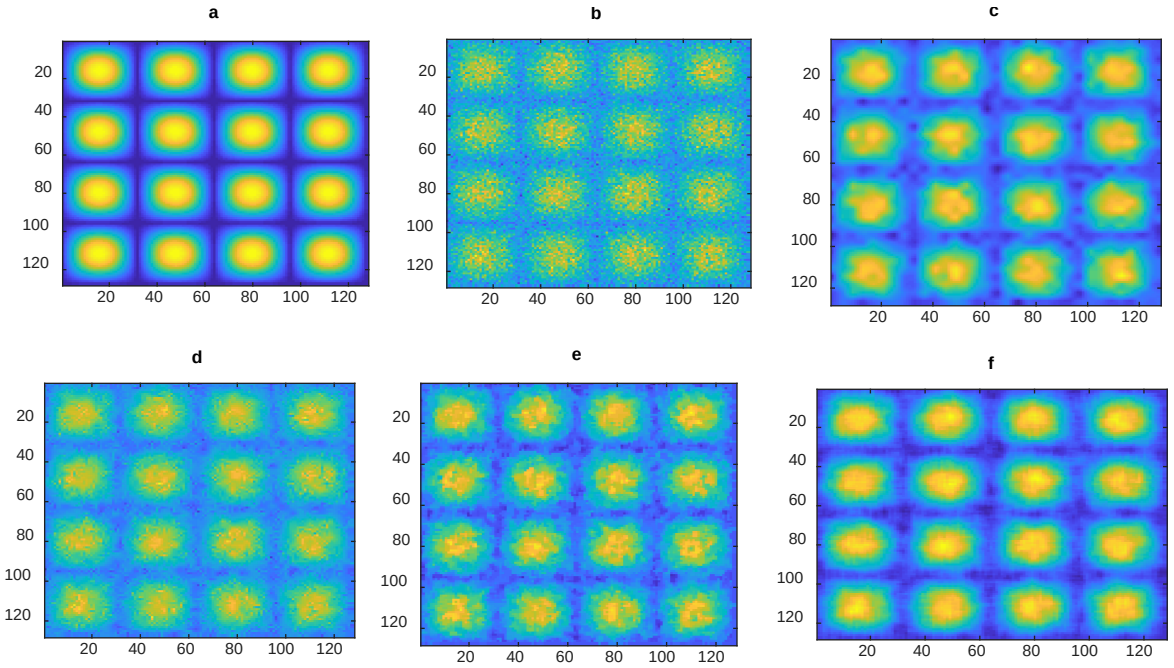

Fig. 4. Comparison of different denoising techniques on Sinsin Image. a) Original images. b) Input Noisy image. c) Denoised image using conventional wavelet-based universal thresholding [27,28]. d) Denoised image using Proposed modified wavelet-based universal thresholding. e) Denoised image using median filter [13–15]. f) Denoised image using averaging filtering [16,17].

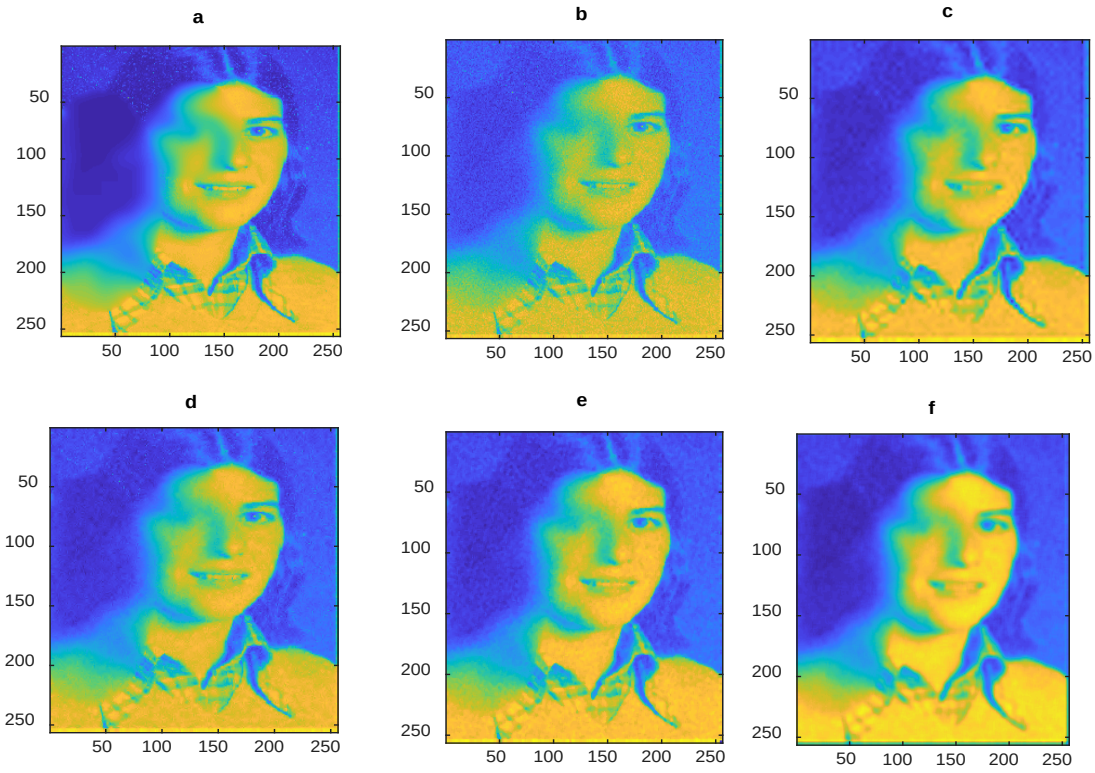

Fig. 5. Comparison of different denoising techniques on Cathe_1 Image. a) Original images. b) Input Noisy image. c) Denoised image using conventional wavelet-based universal thresholding [27,28]. d) Denoised image using Proposed modified wavelet-based universal thresholding. e) Denoised image using median filter [13–15]. f) Denoised image using averaging filtering [16,17].

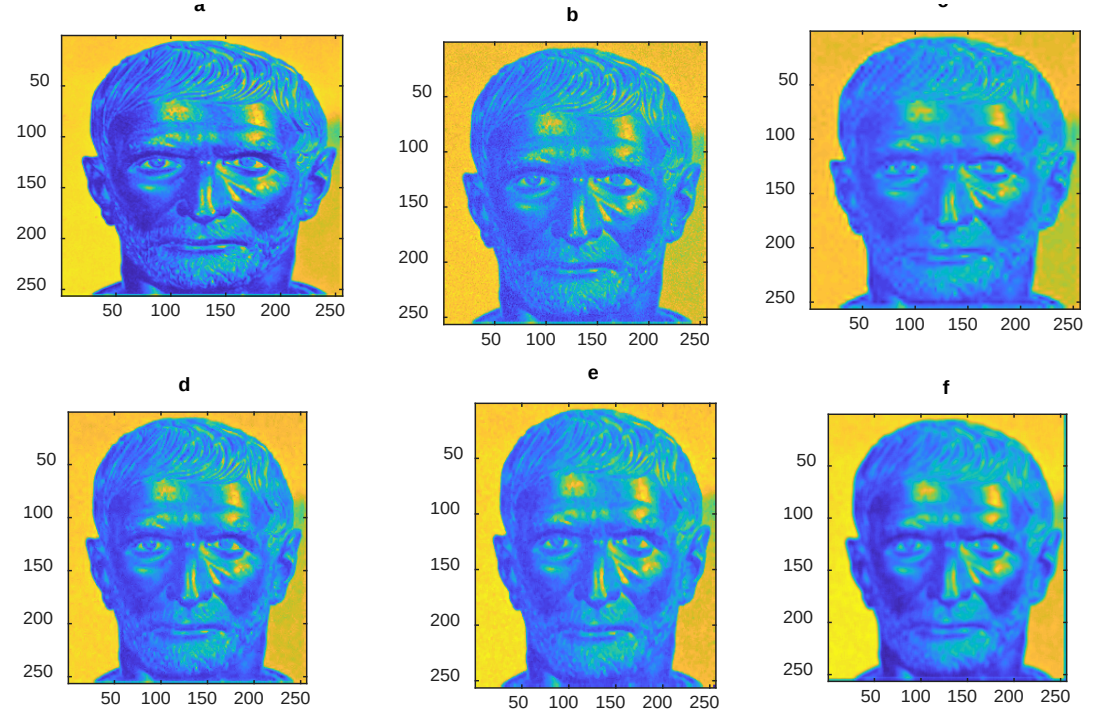

Fig. 6. Comparison of different denoising techniques on Bust Image. a) Original images. b) Input Noisy image. c) Denoised image using conventional wavelet-based universal thresholding [27,28]. d) Denoised image using Proposed modified wavelet-based universal thresholding. e) Denoised image using median filter [13–15]. f) Denoised image using averaging filtering [16,17].

In order to appraise the qualities of the images obtained and displayed in Figs. 2-6 using the proposed wavelet-based thresholding results compared to other standard techniques, we engaged seven performance indicators: RMSE, MAE, SC, PSNR, SSIM, SRER, NIQE, and BRISQUE. The first five indicators, RMSE, MAE, SC, PSNR, SSIM, and SRER, are reference indicators. The remaining two indicators, the NIQE and BRISQUE, are referenceless. The normalized image length is used instead of the actual image length to bring the pixel intensity and the employed indicators values to the range that is more normal and clear to the senses. The results show that the image qualities expressed in RMSE, MAE, PSNR, SSIM, NIQE, SRER, and BRISQUE decrease as image length increases.

For the superior performance of the proposed wavelet threshold algorithm, the PSNR, SSIM, and SRER must be higher, while lower values of NIQE, BRISQUE, RMSE, and MAE are preferred. Figs. 7 to 9 show the PSNR, SSIM, and SRER quantified performance behavior versus normalized image length using the proposed modified wavelet-based universal thresholding (MWUT) rule and the conventional wavelet-based universal thresholding (CWUT) rule, median filter, and averaging filter. The normalized image length is used instead of the real length to reduce the feature space and clarify the range of performance indicators values to the senses.

As seen in Figs. 7 to 9, higher PSNR, SSIM, and SRER values in each graph show the superior denoising performance of our modified wavelet-based universal thresholding technique over others. Similarly, in Figs. 7 to 9, lower NIQE, BRISQUE, RMSE, and MAE values indicate higher and better image quality results using the proposed modified wavelet-based universal thresholding technique.

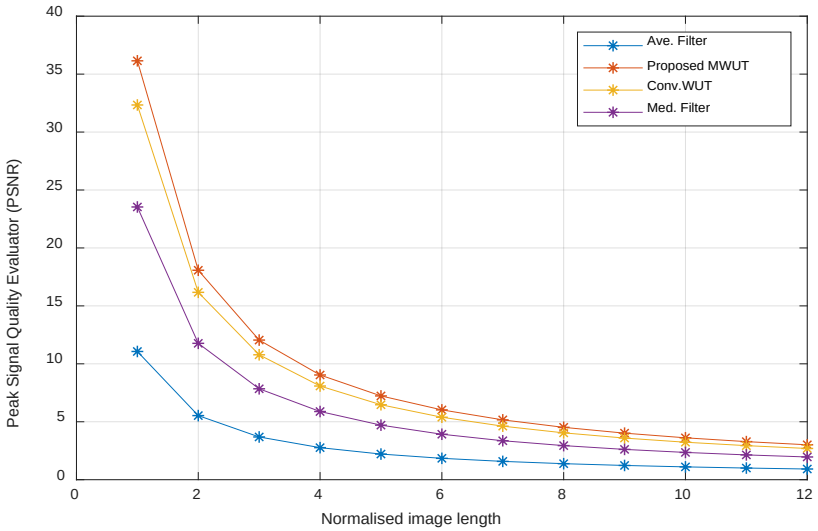

Fig. 7. PSNR performance results from comparing different denoising techniques on Mask Image: Conv.WUT-Denoised image result using conventional wavelet-based universal thresholding [27,28]; MWUT-Denoised image result using Proposed modified wavelet-based universal thresholding; Med.Filter-Denoised image result using median filter [13–15]; Ave.Filter-Denoised image result using averaging filtering [16,17].

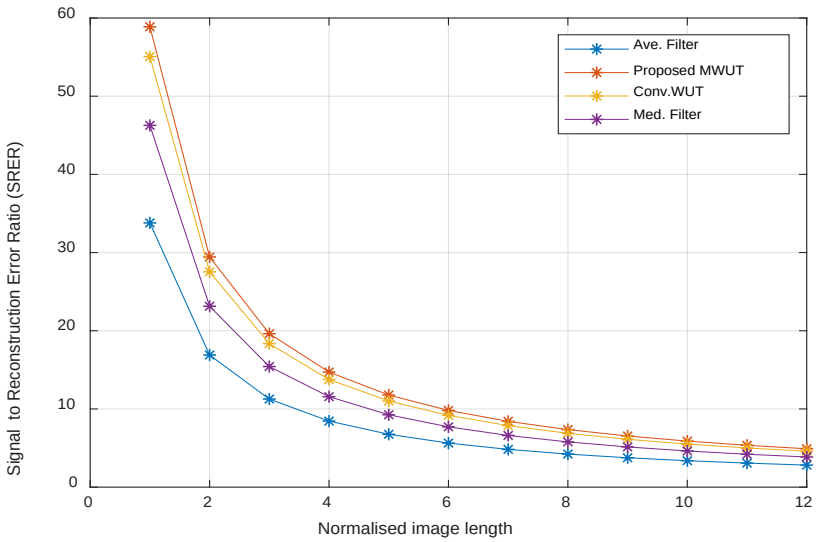

Fig. 8. SRER performance results from comparing different denoising techniques on Mask Image: Conv.WUT-Denoised image result using conventional wavelet-based universal thresholding [27,28]; MWUT-Denoised image result using Proposed modified wavelet-based universal thresholding; Med.Filter-Denoised image result using median filter [13–15]; Ave.Filter-Denoised image result using averaging filtering [16,17].

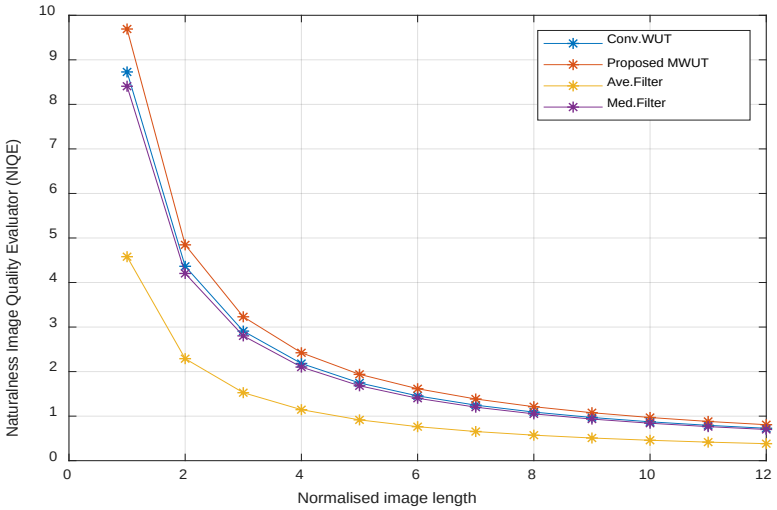

Fig. 9. NIQE performance results from comparing different denoising techniques on Mask Image: Conv.WUT-Denoised image result using conventional wavelet-based universal thresholding [27,28]; MWUT-Denoised image result using Proposed modified wavelet-based universal thresholding; Med.Filter-Denoised image result using median filter [13–15]; Ave.Filter-Denoised image result using averaging filtering [16,17].

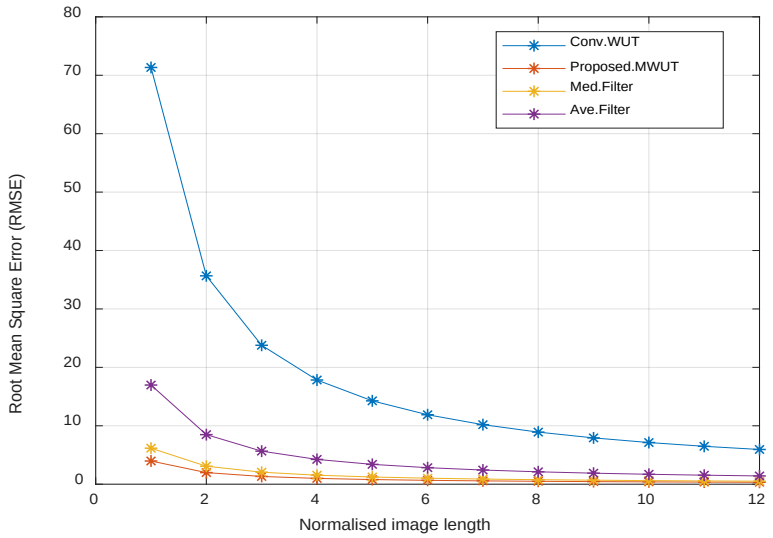

Fig. 10. RMSE performance results from comparing different denoising techniques on Mask Image: Conv.WUT-Denoised image result using conventional wavelet-based universal thresholding [27,28].; MWUT-Denoised image result using Proposed modified wavelet-based universal thresholding; Med.Filter-Denoised image result using median filter [13–15]; Ave.Filter-Denoised image result using averaging filtering [16,17].

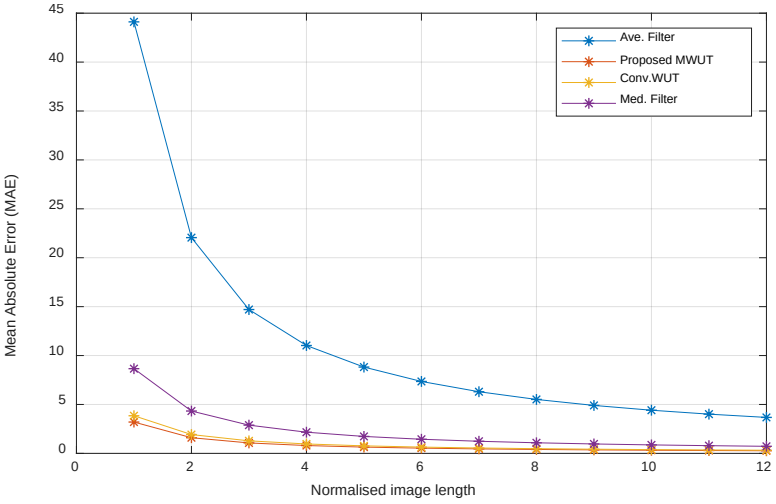

Fig.11. MAE performance results from comparing different denoising techniques on Mask Image: Conv.WUT-Denoised image result using conventional wavelet-based universal thresholding [27,28]; MWUT-Denoised image result using Proposed modified wavelet-based universal thresholding; Med.Filter-Denoised image result using median filter [13–15]; Ave.Filter-Denoised image result using averaging filtering [16,17].

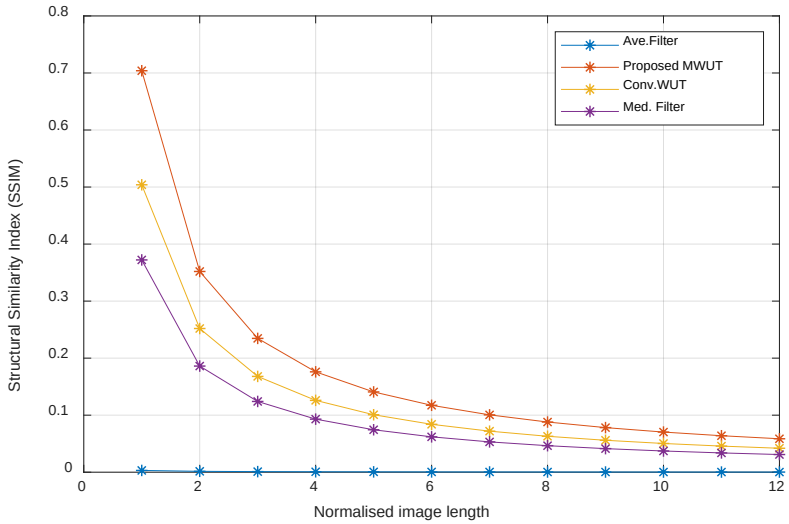

Fig. 12. SSIM performance results from comparing different denoising techniques on Mask Image: Conv.WUT-Denoised image result using conventional wavelet-based universal thresholding [27,28]; MWUT-Denoised image result using Proposed modified wavelet-based universal thresholding; Med.Filter-Denoised image result using median filter [13–15]; Ave.Filter-Denoised image result using averaging filtering [16,17].

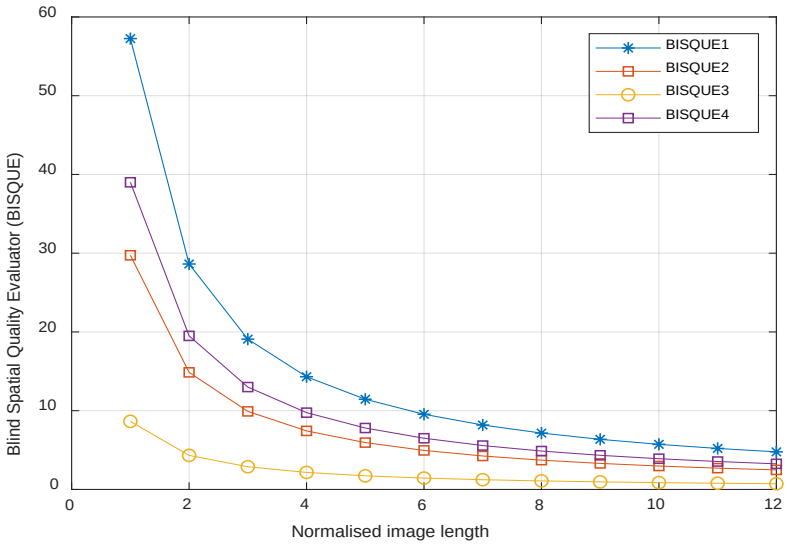

Fig. 13. BISQUE performance results from comparing different denoising techniques on Mask Image: Conv.WUT-Denoised image result using conventional wavelet-based universal thresholding [27,28]; MWUT-Denoised image result using Proposed modified wavelet-based universal thresholding; Med.Filter-Denoised image result using median filter [13–15]; Ave.Filter-Denoised image result using averaging filtering [16,17].

The mean quantitative results of the employed performance parameters are provided in Tables 1 to 4 for clarity purposes. Again, the proposed MWUT approach upturns other methods by providing better-denoised mask, mandrill, sinsin, Cathe_1, and Bust image qualities. For example, in terms of PSNR quality, as provided in Table 1, the proposed MWUT method attained 36.23, 26.01, 35.91, 34.47, and 33.06 values for the five processed images, is relatively higher and better than the standard denoising methods employed for benchmarking. The best performance of the proposed MWUT approach can be ascribed to its capacity to optimally denoise the degraded noisy images with both uniform and non-uniform variations in illumination and contrast. The disadvantages of other filters reside in their inability to mollify medium-tailed and related noise distributions.

Table 1. Performance comparison of proposed denoising technique and other conventional techniques on Mask, Mandrill, Sinsin, Cathe_1, and Bust Images with 5dB noise variance

Method	Mask	Mandrill	Sinsin	Cathe_1	Bust
	RMSE Values				
Conv.WUT	71.37	83.08	5.65	9.08	12.07
Prop.WUT	3.95	12.82	4.10	4.84	5.69
Med.Filter	6.15	26.97	4.79	10.75	9.85
Ave.Filter	16.98	33.65	5.27	15.01	19.67
	MAE Values				
Conv.WUT	44.18	68.37	4.49	6.47	8.93
Prop.WUT	3.19	10.24	3.31	3.85	4.56
Med.Filter	3.84	16.73	3.43	5.72	5.88
Ave.Filter	8.65	24.24	4.19	8.30	12.40
	PNSR Values				
Conv.WUT	11.09	9.77	33.12	29.01	26.53
Prop.WUT	36.23	26.01	35.91	34.47	33.06
Med.Filter	32.38	19.55	34.57	27.53	28.29
Ave.Filter	23.56	17.62	33.73	24.64	22.29
	SRER Values				
Conv.WUT	33.79	35.61	42.85	48.97	47.39
Prop.WUT	58.93	51.85	45.63	54.44	53.91
Med.Filter	55.08	45.39	44.29	47.50	49.15
Ave.Filter	46.26	43.46	43.45	44.60	43.14
	NIQE Values				
Conv.WUT	9.31	7.73	18.87	8.42	11.36
Prop.WUT	12.18	6.34	18.87	8.30	5.10
Med.Filter	4.31	4.48	18.87	4.36	4.92
Ave.Filter	7.67	6.64	18.87	9.89	6.25
	SSIM Values				
Conv.WUT	0.01	0.01	0.77	0.43	0.52
Prop.WUT	0.71	0.78	0.87	0.74	0.76
Med.Filter	0.51	0.52	0.83	0.46	0.64
Ave.Filter	0.38	0.26	0.79	0.32	0.37
	BRISQUE Values				
Conv.WUT	56.63	45.07	43.47	65.62	52.05
Prop.WUT	29.66	25.67	45.08	19.97	40.54
Med.Filter	10.34	38.62	39.39	17.12	34.11
Ave.Filter	39.63	40.40	43.58	36.68	42.02

Table 2. Performance comparison of proposed denoising technique and other conventional techniques on Mask, Mandrill, Sinsin, Cathe_1, and Bust Images with 10dB noise variance

Method	Mask	Mandrill	Sinsin	Cathe_1	Bust
	RMSE Values				
Conv.WUT	71.78	83.49	10.60	13.10	16.00
Prop.WUT	7.41	14.78	7.40	8.01	8.91
Med.Filter	10.45	28.20	9.62	13.70	13.02
Ave.Filter	19.01	34.71	9.99	17.22	21.43
	MAE Values				
Conv.WUT	45.66	68.68	8.45	9.94	12.26
Prop.WUT	5.98	11.88	5.98	6.44	7.19
Med.Filter	7.37	18.32	7.11	8.85	8.83
Ave.Filter	11.86	25.48	7.96	11.30	14.71
	PNSR Values				
Conv.WUT	11.04	9.73	27.66	25.82	24.08
Prop.WUT	30.77	24.77	30.78	30.10	29.17
Med.Filter	27.78	19.16	28.50	25.43	25.87
Ave.Filter	22.59	17.36	28.17	23.44	21.55
	SRER Values				
Conv.WUT	33.74	35.57	37.37	45.78	44.94
Prop.WUT	53.47	50.61	40.50	50.06	50.03
Med.Filter	50.48	45.00	38.22	45.40	46.73
Ave.Filter	45.28	43.20	37.89	43.41	42.40
	NIQE Values				
Conv.WUT	11.12	8.61	18.87	9.67	12.43
Prop.WUT	16.15	6.37	18.87	16.56	6.78
Med.Filter	4.52	4.47	18.88	4.39	4.56
Ave.Filter	9.62	7.11	18.87	9.19	6.86
	SSIM Values				
Conv.WUT	-0.00	0.01	0.52	0.31	0.40
Prop.WUT	0.67	0.75	0.76	0.68	0.73

Med.Filter	0.39	0.49	0.60	0.36	0.54
Ave.Filter	0.27	0.24	0.55	0.22	0.31
	BRISQUE Values				
Conv.WUT	52.69	45.52	44.71	59.76	46.42
Prop.WUT	32.39	27.36	37.74	31.53	48.94
Med.Filter	4.65	32.68	36.97	13.22	31.02
Ave.Filter	36.03	40.11	43.48	23.74	40.99

Table 3. Performance comparison of proposed denoising technique and other conventional techniques on Mask, Mandrill, Sinsin Cathe_1, and Bust Images with 15dB noise variance

Method	Mask	Mandrill	Sinsin	Cathe_1	Bust
	RMSE Values				
Conv.WUT	72.68	84.13	15.71	17.33	19.97
Prop.WUT	10.83	17.33	11.08	11.35	12.16
Med.Filter	15.14	30.24	14.63	17.48	17.01
Ave.Filter	21.94	36.42	14.93	20.39	24.05
	MAE Values				
Prop.WUT	47.57	69.14	12.55	13.49	15.56
Med.Filter	8.77	13.98	8.94	9.15	9.83
Ave.Filter	11.00	20.47	10.88	12.21	12.08
Conv.WUT	15.30	27.29	11.90	14.66	17.51
	PNSR Values				
Conv.WUT	10.94	9.67	24.24	23.39	22.16
Prop.WUT	27.47	23.39	27.27	27.07	26.46
Med.Filter	24.56	18.55	24.86	23.32	23.55
Ave.Filter	21.34	16.94	24.68	21.97	20.54
	SRER Values				
Conv.WUT	33.64	35.51	33.96	43.35	43.02
Prop.WUT	50.17	49.23	37.00	47.03	47.32
Med.Filter	47.26	44.39	34.58	43.28	44.41
Ave.Filter	44.04	42.78	34.40	41.94	41.41
	NIQE Values				
Conv.WUT	14.06	9.35	18.87	10.30	13.82
Prop.WUT	16.06	7.42	18.88	17.58	8.58
Med.Filter	4.98	4.73	18.88	5.19	4.60
Ave.Filter	11.99	7.66	18.87	10.92	7.52
	SSIM Values				
Conv.WUT	-0.01	0.00	0.35	0.24	0.34
Prop.WUT	0.65	0.73	0.67	0.64	0.70
Med.Filter	0.34	0.45	0.44	0.30	0.47
Ave.Filter	0.22	0.21	0.37	0.17	0.27
	BRISQUE Values				
Conv.WUT	49.47	45.35	45.03	55.14	44.15
Prop.WUT	26.81	30.32	28.96	31.67	50.18
Med.Filter	7.90	32.01	17.39	12.32	28.60
Ave.Filter	42.76	39.73	44.21	26.71	39.39

Table 4. Performance comparison of proposed denoising technique and other conventional techniques on Mask, Mandrill, Sinsin, Cathe_1 and Bust Images with 20dB noise variance

Method	Mask	Mandrill	Sinsin	Cathe_1	Bust
	RMSE Values				
Conv.WUT	73.64	85.14	20.91	21.78	24.09
Prop.WUT	14.25	20.03	14.55	14.66	15.45
Med.Filter	19.90	32.97	19.54	21.93	21.44
Ave.Filter	25.48	38.71	19.82	24.25	27.32
	MAE Values				
Conv.WUT	49.40	69.88	16.66	17.14	18.96
Prop.WUT	11.54	16.19	11.77	11.85	12.50
Med.Filter	14.62	22.96	14.58	15.76	15.57
Ave.Filter	18.81	29.48	15.78	18.23	20.59
	PNSR Values				
Conv.WUT	10.82	9.56	21.76	21.40	20.53
Prop.WUT	25.09	22.13	24.91	24.84	24.39
Med.Filter	22.19	17.80	22.34	21.34	21.54
Ave.Filter	20.04	16.41	22.22	20.47	19.43
	SRER Values				
Conv.WUT	33.52	35.40	31.49	41.37	41.39
Prop.WUT	47.79	47.97	34.64	44.81	45.25
Med.Filter	44.88	43.64	32.07	41.31	42.40

Ave.Filter	42.74	42.25	31.95	40.44	40.29
	NIQE Values				
Conv.WUT	15.90	10.47	18.88	10.90	13.80
Prop.WUT	15.03	7.86	18.88	12.94	8.61
Med.Filter	5.80	4.24	18.88	4.98	6.42
Ave.Filter	11.81	8.40	18.87	11.92	8.19
	SSIM Values				
Conv.WUT	-0.00	0.01	0.24	0.20	0.29
Prop.WUT	0.63	0.72	0.62	0.62	0.68
Med.Filter	0.31	0.42	0.34	0.26	0.41
Ave.Filter	0.18	0.19	0.27	0.13	0.23
	BRISQUE Values				
Conv.WUT	47.29	45.30	52.65	51.71	43.87
Prop.WUT	28.23	32.95	34.50	32.21	49.48
Med.Filter	14.64	33.02	29.03	19.99	22.21
Ave.Filter	43.52	39.54	41.65	29.25	40.07

5. Conclusion

In this paper, a modified wavelet-based universal thresholding technique has been proposed to enhance noisy image denoising. Compared with three state-of-the-art denoising techniques, the proposed method denoised four different noisy images. In order to qualitatively ascertain the performance of the proposed denoising method over other contenders, seven performance indicators such as RMSE, MAE, SC, PSNR, SSIM, SRER, NIQE, and BRISQUE, were employed, and all indicators are graphically and qualitatively highlighted. The higher PSNR, SSIM, and SRER in the final results show the superior denoising performance of our modified wavelet-based universal thresholding technique over the preliminaries. Similarly, lower NIQE, BRISQUE, RMSE, and MAE values in the final results indicate higher and better image quality using the proposed wavelet-based universal thresholding technique over the existing three state-of-the-art denoising techniques. The projected results would find practical applications in digital image processing and enhancement. Our future work will optimize the proposed wavelet-based universal thresholding technique for efficient performance. Finally, future work would also explore efficient algorithms for intelligent signal processing enabled by pervasive artificial intelligence to benefit the next generation of wireless communication systems.

Abbreviations

BRISQUE	Blind/Referenceless Image Spatial Quality Evaluator
CWUT	Conventional Wavelet-based Universal Thresholding
MAE	Mean Absolute Error
MWUT	Modified Wavelet-based Universal Thresholding
NIQE	Blind Spatial Quality Evaluator
PSNR	Peak Signal-to-Noise Ratio
RMSE	Root Mean Square Error
SC	Structural Content
SRER	Signal-to-Reconstruction-Error Ratio
SSIM	Structural Similarity Index Method

Availability of data and material

The data that support the findings of this study are available from the corresponding author upon reasonable request.

Competing interests

The authors declare that they have no conflicts of interest.

Acknowledgment

The authors thank the anonymous reviewers for their valuable comments which helped to improve the quality of the manuscript.

Funding Statement

The work of Agbotiname Lucky Imoize is supported in part by the Nigerian Petroleum Technology Development Fund (PTDF) and in part by the German Academic Exchange Service (DAAD) through the Nigerian-German Postgraduate Program under Grant 57473408.

References

[1] X. Zhu, P. Milanfar, Automatic parameter selection for denoising algorithms using a no-reference measure of image content, IEEE Trans. Image Process. 19 (2010) 3116–3132.

[2] Y. Qian, Image denoising algorithm based on improved wavelet threshold function and median filter, in: 2018 IEEE 18th Int. Conf. Commun. Technol., IEEE, 2018: pp. 1197–1202.

[3] G. Deng, Z. Liu, A wavelet image denoising based on the new threshold function, in: 2015 11th Int. Conf. Comput. Intell. Secur., IEEE, 2015: pp. 158–161.

[4] Z. Jianhua, Z. Qiang, Z. Jinrong, S. Lin, W. Jilong, A novel algorithm for threshold image denoising based on wavelet construction, Cluster Comput. 22 (2019) 12443–12450.

[5] M.A. Adelabu, A.L. Imoize, K.E. Adesoji, Enhancement of a Camera-Based Continuous Heart Rate Measurement Algorithm, SN Comput. Sci. 3 (2022) 284. https://doi.org/10.1007/s42979-022-01179-w.

[6] T. Dixit, N. Singh, Proposing a Framework to Analyze Breast Cancer in Mammogram Images Using Global Thresholding, Gray Level Co‐Occurrence Matrix, and Convolutional Neural Network (CNN), Adv. Data Sci. Anal. Concepts Paradig. (2023) 145–180.

[7] J. Isabona, Wavelet Generalized Regression Neural Network Approach for Robust Field Strength Prediction, Wirel. Pers. Commun. 114 (2020) 3635–3653. https://doi.org/10.1007/s11277-020-07550-5.

[8] J. Isabona, R. Kehinde, Multi-resolution based discrete wavelet transform for enhanced signal coverage processing and prediction analysis, FUDMA J. Sci. 3 (2019) 6–15.

[9] C. Ebhota, J. Isabona, V.M. Srivastava, Improved adaptive signal power loss prediction using combined vector statistics based smoothing and neural network approach, Prog. Electromagn. Res. C. 82 (2018) 155–169. https://doi.org/10.2528/pierc18011203.

[10] P.-L. Shui, Image denoising algorithm via doubly local Wiener filtering with directional windows in wavelet domain, IEEE Signal Process. Lett. 12 (2005) 681–684.

[11] A. Foi, V. Katkovnik, K. Egiazarian, Signal-dependent noise removal in pointwise shape-adaptive DCT domain with locally adaptive variance, in: 2007 15th Eur. Signal Process. Conf., IEEE, 2007: pp. 2159–2163.

[12] S. Solbo, T. Eltoft, Homomorphic wavelet-based statistical despeckling of SAR images, IEEE Trans. Geosci. Remote Sens. 42 (2004) 711–721.

[13] H.-L. Eng, K.-K. Ma, Noise adaptive soft-switching median filter for image denoising, in: 2000 IEEE Int. Conf. Acoust. Speech, Signal Process. Proc. (Cat. No. 00CH37100), IEEE, 2000: pp. 2175–2178.

[14] H.-L. Eng, K.-K. Ma, Noise adaptive soft-switching median filter, IEEE Trans. Image Process. 10 (2001) 242–251.

[15] K.E. Barner, G.R. Arce, Nonlinear signal and image processing: theory, methods, and applications, CRC Press, 2003.

[16] L. Fan, F. Zhang, H. Fan, C. Zhang, Brief review of image denoising techniques, Vis. Comput. Ind. Biomed. Art. 2 (2019) 1–12.

[17] R. C. Gonzalez, R. E. Woods, S. L. Eddins, Digital Image Processing Using Matlab, 2004.

[18] X. Liu, M. Tanaka, M. Okutomi, Single-image noise level estimation for blind denoising, IEEE Trans. Image Process. 22 (2013) 5226–5237.

[19] X. Liu, M. Tanaka, M. Okutomi, Signal dependent noise removal from a single image, in: 2014 IEEE Int. Conf. Image Process., IEEE, 2014: pp. 2679–2683.

[20] M.A. Adelabu, A.L. Imoize, G.U. Ughegbe, Performance Evaluation of Radio Frequency Interference Measurements from Microwave Links in Dense Urban Cities, Telecom. 2 (2021) 328–368. https://doi.org/10.3390/telecom2040021.

[21] G.U. Ughegbe, M.A. Adelabu, A.L. Imoize, Experimental data on radio frequency interference in microwave links using frequency scan measurements at 6 GHz, 7 GHz, and 8 GHz, Data Br. 35 (2021) 106916. https://doi.org/10.1016/j.dib.2021.106916.

[22] E. Srinivasan, D. Ebenezer, New Nonlinear Filtering Strategies for eliminating Medium and Long tailed noise in images with edge preservation properties, IETE J. Educ. 46 (2005) 3–11.

[23] L.J. Halliwell, Classifying the tails of loss distributions, Casualty Actuar. Soc. 2 (2013) 1–27.

[24] F. Ming, H. Long, Partial discharge de-noising based on hybrid particle swarm optimization SWT adaptive threshold, IEEE Access. (2023).

[25] X. Qiao, J. Bao, H. Zhang, L. Zeng, D. Li, Underwater image quality enhancement of sea cucumbers based on improved histogram equalization and wavelet transform, Inf. Process. Agric. 4 (2017) 206–213. https://doi.org/10.1016/j.inpa.2017.06.001.

[26] K.V.N. Kavitha, S. Ashok, A.L. Imoize, S. Ojo, K.S. Selvan, T.A. Ahanger, M. Alhassan, On the Use of Wavelet Domain and Machine Learning for the Analysis of Epileptic Seizure Detection from EEG Signals, J. Healthc. Eng. 2022 (2022) 8928021. https://doi.org/10.1155/2022/8928021.

[27] D.L. Donoho, J.M. Johnstone, Ideal spatial adaptation by wavelet shrinkage, Biometrika. 81 (1994) 425–455.

[28] D.L. Donoho, I.M. Johnstone, Adapting to unknown smoothness via wavelet shrinkage, J. Am. Stat. Assoc. 90 (1995) 1200–1224.

[29] A.S. Dixit, P. Sharma, A Comparative Study of Wavelet Thresholding for Image Denoising, Int. J. Image, Graph. Signal Process, vol.6, no.12, pp.39-46, 2014.

[30] X. Wang, X. Ou, B.-W. Chen, M. Kim, Image denoising based on improved wavelet threshold function for wireless camera networks and transmissions, Int. J. Distrib. Sens. Networks. 11 (2015) 670216.

[31] C.F. Cunha, M.R. Petraglia, A.T. Carvalho, A.C.S. Lima, A Wavelet Threshold Function for Treatment of Partial Discharge Measurements, in: Wavelet Theory, IntechOpen, 2020.

[32] B. Xie, Z. Xiong, Z. Wang, L. Zhang, D. Zhang, F. Li, Gamma spectrum denoising method based on improved wavelet threshold, Nucl. Eng. Technol. 52 (2020) 1771–1776.

[33] K.V.N. Kavitha, A. Shanmugam, A.L. Imoize, Optimized deep knowledge-based no-reference image quality index for denoised MRI images, Sci. African. 20 (2023) e01680.

[34] A.S. Akinfende, A.L. Imoize, O.S. Ajose, Investigation of iris segmentation techniques using active contours for non-cooperative iris recognition, Indones. J. Electr. Eng. Comput. Sci. 19 (2020) 1275–1286.
[35] P. Singhai, A. Kumar, A. Ateek, I.A. Ansari, G.K. Singh, H.N. Lee, ECG Signal Compression Based on Optimization of Wavelet Parameters and Threshold Levels Using Evolutionary Techniques, Circuits, Syst. Signal Process. (2023) 1–29.
[36] S.O. Ajose, A.L. Imoize, Propagation measurements and modelling at 1800 MHz in Lagos Nigeria, Int. J. Wirel. Mob. Comput. 6 (2013) 165–174. https://doi.org/10.1504/IJWMC.2013.054042.
[37] A.L. Imoize, A.E. Ibhaze, P.O. Nwosu, S.O. Ajose, Determination of Best-fit Propagation Models for Pathloss Prediction of a 4G LTE Network in Suburban and Urban Areas of Lagos, Nigeria, West Indian J. Eng. 41 (2019) 13–21.
[38] A.E. Ibhaze, A.L. Imoize, S.O. Ajose, S.N. John, C.U. Ndujiuba, F.E. Idachaba, An Empirical Propagation Model for Path Loss Prediction at 2100MHz in a Dense Urban Environment, Indian J. Sci. Technol. 10 (2017) 1–9. https://doi.org/10.17485/ijst/2017/v10i5/90654.
[39] D.O. Ojuh, J. Isabona, Optimum signal denoising based on wavelet shrinkage thresholding techniques: white Gaussian noise and white uniform noise case study, J. Sci. Eng. Res. 5 (2018) 179–186.
[40] V.C. Ebhota, J. Isabona, V.M. Srivastava, Environment-Adaptation Based Hybrid Neural Network Predictor for Signal Propagation Loss Prediction in Cluttered and Open Urban Microcells, Wirel. Pers. Commun. 104 (2019) 935–948. https://doi.org/10.1007/s11277-018-6061-2.
[41] I.K. Okakwu, E.S. Oluwasogo, A.E. Ibhaze, A.L. Imoize, A comparative study of time series analysis for forecasting energy demand in Nigeria, Niger. J. Technol. 38 (2019) 465. https://doi.org/10.4314/njt.v38i2.24.
[42] F. Memon, M.A. Unar, S. Memon, Image quality assessment for performance evaluation of focus measure operators, Mehran Univ. Res. J. Eng. Technol. 34 (2015) 379–386.
[43] A. Sabir, K. Khurshid, A. Salman, Segmentation-based image defogging using modified dark channel prior, EURASIP J. Image Video Process. 2020 (2020) 1–14.
[44] Z. Wang, A.C. Bovik, H.R. Sheikh, E.P. Simoncelli, Image quality assessment: from error visibility to structural similarity, IEEE Trans. Image Process. 13 (2004) 600–612.
[45] A. Mittal, R. Soundararajan, A.C. Bovik, Making a “completely blind” image quality analyzer, IEEE Signal Process. Lett. 20 (2012) 209–212.
[46] A. Mittal, A.K. Moorthy, A.C. Bovik, No-reference image quality assessment in the spatial domain, IEEE Trans. Image Process. 21 (2012) 4695–4708.
[47] G. Wang, Y. Zhang, W.-F. Xie, Y. Qu, L. Feng, Hyperspectral linear unmixing based on collaborative sparsity and multi-band non-local total variation, Int. J. Remote Sens. 43 (2022) 1–26.
[48] U. Sara, M. Akter, M.S. Uddin, Image quality assessment through FSIM, SSIM, MSE and PSNR—a comparative study, J. Comput. Commun. 7 (2019) 8–18.
[49] A. Mittal, A.K. Moorthy, A.C. Bovik, Blind/referenceless image spatial quality evaluator, in: 2011 Conf. Rec. Forty Fifth Asilomar Conf. Signals, Syst. Comput., IEEE, 2011: pp. 723–727.
[50] J. Isabona, D.O. Ojuh, Wavelet selection based on wavelet transform for optimum noisy signal processing, Int. J. Basic Appl. Sci. 3 (2017) 57–65.

Authors’ Profiles

Joseph Isabona received Ph.D. and M.Sc. degrees in Communication Electronics in 2013 and 2007, respectively, and a B.Sc in Applied Physics in 2003. He is the Author of more than 150 scientific contributions, including articles in international refereed journals and conferences in wireless mobile communications. The Author is a Postdoctoral Research Fellow of the Department of Electronic Engineering, Howard College, University of KwaZulu-Natal, Durban, South Africa. His interest areas include Signal Processing, RF Propagation Modelling, and Radio Resource Management.

Agbotiname Lucky Imoize is a lecturer in the Department of Electrical and Electronics Engineering at the University of Lagos, Nigeria. His research interests cover the fields of 6G wireless communication, wireless security systems, and artificial intelligence. He is a registered engineer with the Council for the Regulation of Engineering in Nigeria (COREN), the Vice Chair of the IEEE Communication Society, Nigeria chapter, a Fulbright research fellow, and a senior member of the IEEE.

Stephen Ojo (Member, IEEE) is a lecturer in the Department of Electrical and Computer Engineering, College of Engineering, Anderson University, Anderson, South Carolina, USA. He received B.Eng (Honours) in Electrical and Electronics Engineering from the Federal University of Technology Akure Nigeria in 2014, M.Sc in Electrical and Electronics Engineering from Girne American University, Cyprus, in 2018, and Ph.D. in Information Systems in May 2021 from the same University. Before Joining Anderson University, he was a Lecturer at Girne American University Cyprus, where he taught courses in distributed computing, advanced programming, and Electric Circuits. Dr. Ojo also worked as a research scholar at Vodafone Telecommunication Company, Cyprus, where he developed a multiplicative-based model for signal propagation in wireless networks. Dr. Ojo was awarded a Mobil scholarship

throughout his undergraduate program. His Ph.D. program also received full sponsorship. Dr. Ojo is a full-time faculty member at Anderson University, the USA, teaching computer programming, electric circuits, machine learning, and artificial intelligence in biomedical applications. He is presently a committee member on the graduate certificate program on ML/AI at the College of Engineering. He is also a member of the curriculum development committee and a member of the faculty search committee. He has authored and co-authored over 30 peer-reviewed papers in journals and conferences. His research interests are wireless networks, machine learning and AI in biomedical devices, and systems modeling.

How to cite this paper: Joseph Isabona, Agbotiname Lucky Imoize, Stephen Ojo, "Image Denoising based on Enhanced Wavelet Global Thresholding Using Intelligent Signal Processing Algorithm", International Journal of Image, Graphics and Signal Processing(IJIGSP), Vol.15, No.5, pp. 1-16, 2023. DOI:10.5815/ijigsp.2023.05.01